Implication of RNA Structure on Antisense Oligonucleotide Hybridization Kinetics

Walt F. Lima, Brett P. Monia, David J. Ecker, and Susan M. Freier*

Department of Molecular and Cellular Biology, Isis Pharmaceuticals, 2280 Faraday Avenue, Carlsbad, California 92008

Received July 8, 1992; Revised Manuscript Received September 18, 1992

ABSTRACT: A 47-nucleotide transcript of the activated Ha-*ras* gene was prepared and determined, by enzymatic structure mapping, to form a stable hairpin structure. Six antisense decaribonucleotides were designed, and association constants (K_a) for the hairpin- and length-matched complements were measured. Two of the antisense oligonucleotides targeted to the loop had nearly equal affinity for the transcript compared to the complement. The others, including one oligonucleotide complementary to the 3′ side of the single-stranded loop, bound 10^5–10^6-fold less tightly to the transcript than to the short complement. We propose the difference in affinity is due to the target structure, both the secondary structure of the stem and the structure in the loop. Measurement of the bimolecular association rate constant, k_1, and the dissociation rate constant, k_{-1}, for these oligonucleotides indicates the observed relationship between affinity and structure is primarily due to k_1.

The proposed mechanism of action of antisense oligonucleotides requires hybridization of an oligonucleotide to its complementary sequence in the RNA target, typically mRNA. Therefore, for an antisense oligonucleotide to be effective, the complementary target sequence must be available for hybridization. Unfortunately, the RNA target is not a single-stranded random coil but contains secondary and tertiary structures. Target RNA structure has been shown to affect the affinity and rates of oligonucleotide hybridization (Freier & Tinoco, 1975; Uhlenbeck, 1972; Yoon et al., 1975; Fedor & Uhlenbeck, 1990; Herschlag & Cech, 1990a,b) as well as the efficacy of antisense oligonucleotides (Bacon & Wickstrom, 1991; Wickstrom et al., 1986; Chiang et al., 1991). Therefore, designing antisense oligonucleotides to take advantage of mRNA structure requires insight into the influence of this structure on oligonucleotide hybridization.

To investigate the effect of hairpin structure on the hybridization of antisense oligonucleotides, an RNA transcript corresponding to residues +18 to +64 of activated Ha-*ras* mRNA (Reddy, 1983) was prepared. This target was chosen for two reasons. First, RNA folding algorithms (Jaeger et al., 1989) predict this region to be folded into a stable hairpin structure. Hairpins are the predominant structure among RNAs whose secondary structure has been characterized (Gutell et al., 1985) and therefore would likely be the structure most frequently associated with an antisense oligonucleotide target site. Second, this fragment contains codon 12, the site of a point mutation thought to be responsible for the transforming activity of mutant Ha-*ras* (Reddy, 1983), and accordingly represents an attractive target for an antisense therapeutic. Therefore, we were interested in evaluating the affinity of antisense oligonucleotides for this target site.

Six antisense decaribonucleotides complementary to various regions of this hairpin were designed and synthesized. Equilibrium and rate constants were determined for hybridization of the 10-mers to the hairpin. Comparison of affinities and rates for hybridization to the hairpin with hybridization to the short single-standed oligoribonucleotide complement shows that the loop structure has a very large effect on hybridization of antisense oligonucleotides. Targeting the 5′ side of the loop results in the greatest hybridization affinity and rate while targeting the 3′ side of the loop results in the lowest affinity. This phenomenon cannot be explained by simple base-pairing thermodynamics.

MATERIALS AND METHODS

Materials. Unlabeled deoxyribonucleoside 5′-triphosphate (dNTP)[1] and NTP, ribonucleases T1 and CL3, and calf intestine alkaline phosphatase were purchased from Boehringer Mannheim (Indianapolis, IN). Ribonucleases A and S1 were from Gibco BRL (Gathersburg, MD). Ribonuclease V1, RNA ligase, and RNAguard were from Pharmacia LKB (Upsalla, Sweden). [γ-^{32}P]ATP and [^{32}P]pCp were from ICN Biochemicals (Irvine, CA) and Amersham (Arlington Heights, IL), respectively. T4 polynucleotide kinase and T7 RNA polymerase were from Promega (Madison, WI). The plasmid pT24-C3, containing the c-Ha-*ras*-1-activated oncogene (codon 12, GGC → GTC), was from American Type Culture Collection (Bethesda, MD). Sep-Pak C18 cartridges were purchased from Waters (Milford, MA). 5′-Dimethoxytrityl 2′-*tert*-butyldimethylsilyl nucleoside 3′-*O*-phosphoramidites were from American Bionetics (Hayward, CA); tetrabutylammonium fluoride was from Aldrich (Milwaukee, WI). Protected phosphoramidites and other standard reagents for chemical synthesis of DNA were purchased from Applied Biosystems Inc. (Foster City, CA).

Preparation of RNA Transcripts. The template for transcription was prepared from the plasmid pT24-C3 using PCR according to standard methods (Ausubel et al., 1989). The sense primer consisted of the 17-mer responsive sequence for the T7 promoter followed by a 15-mer sequence homologous to residues +18 to +32 of the activated Ha-*ras* mRNA sequence. The antisense primer was complementary to residues +50 to +64 of the mRNA sequence. After purification on a 2% agarose gel (Jinno et al., 1988), the template was used to synthesize a 47-base segment of activated Ha-*ras* mRNA containing codon 12. Transcripts were prepared in

[1] Abbreviations: dNTP, deoxyribonucleoside 5′-triphosphate; DTT, dithiothreitol; EDTA, ethylenediaminetetraacetic acid; K_a, association constant; K_d, dissociation constant; k_1, bimolecular association rate constant; k_{-1}, dissociation rate constant; NTP, ribonucleoside triphosphate; PCR, polymerase chain reaction; PEG, poly(ethylene glycol); Y, pyrimidine.

0006-2960/92/0431-12055$03.00/0

100 μL containing 40 mM Tris-HCl, pH 8.1, 22 mM $MgCl_2$, 5 mM DTT, 1 mM spermidine, 0.01% Triton X-100, 4 mM each rNTP, 100 units of RNAguard (RNase inhibitor), 80 mg/mL PEG, 10 nM T7 RNA polymerase, and roughly 1 μg of template. Reactions were incubated at 37 °C for 2 h.

Oligonucleotide Synthesis. Oligoribonucleotides were synthesized using an Applied Biosystems 380B automated DNA synthesizer and 5′-dimethoxytrityl 2′-*tert*-butyldimethylsilyl nucleoside 3′-*O*-phosphoramidites (Wu & Ogilvie, 1990). Protecting groups on the exocyclic amines of A, C, and G were phenoxyacetyl (Wu et al., 1989). The standard DNA synthesis cycle was modified by increasing the wait step after the pulse delivery of tetrazole to 900 s. Oligonucleotides were deprotected by overnight incubation at room temperature in methanolic ammonia. After oligonucleotides were dried in vacuo, the 2′-silyl group was removed by overnight incubation at room temperature in 1 M tetrabutylammonium fluoride in tetrahydrofuran. Oligonucleotides were purified using a C18 Sep-Pak cartridge (Freier et al., 1985; Sambrook et al., 1989) followed by ethanol precipitation. Analytical denaturing polyacrylamide electrophoresis demonstrated the RNA oligonucleotides were greater than 90% full-length material.

DNA oligonucleotides used for PCR primers were synthesized using an Applied Biosystems 380B automated synthesizer and standard phosphoramidite chemistry. Primers were purified by precipitation 2 times out of 0.5 M NaCl with 2.5 volumes of ethanol.

^{32}P Labeling of RNA Transcripts and Oligoribonucleotides. RNA transcripts and oligonucleotides were 5′ end labeled with ^{32}P using [γ-^{32}P]ATP, T4 polynucleotide kinase, and standard procedures (Ausubel et al., 1989). RNA transcripts were 3′ end labeled with ^{32}P using [^{32}P]pCp, T4 RNA ligase, and standard procedures (Ausubel et al., 1989). Labeled oligonucleotides were purified using a C18 Sep-Pak (Freier et al., 1985; Sambrook et al., 1989); labeled transcripts were purified by electrophoresis on a 12% denaturing polyacrylamide gel (Sambrook et al., 1989). Specific activities of the labeled 47-mer and 10-mers were, respectively, about 2000 and about 6000 cpm/fmol.

Enzymatic Structure Mapping. Digestions with RNase T1, V1, CL3, and A were performed in 10 μL containing 10 mM Tris-HCl, pH 7.4, 50 mM NaCl, 5 mM $MgCl_2$, 3 μg of tRNA, and 3.5×10^4 cpm of ^{32}P-labeled transcript. RNase S1 digestions were performed in 10 μL containing 50 mM sodium acetate, pH 5.0, 1 mM zinc acetate, 250 mM NaCl, 3 μg of tRNA, and 3.5×10^4 cpm of ^{32}P-labeled transcript. To guarantee only primary hits were detected, the concentration of each enzyme was chosen such that roughly 90% of the transcript remained intact. Reactions were incubated 5 min at 25 °C except for reactions containing RNase S1 which were incubated 5 min at 4 °C. Following incubation, reactions were quenched by addition of 5 μL of 9 M urea. Reaction products were resolved using a 12% polyacrylamide sequencing gel (Ausubel et al., 1989).

Structures of oligonucleotide-bound transcripts were mapped as described above except oligonucleotide was added for a final concentration of 10 μM and incubated 2 h at 37 °C prior to enzymatic digestion.

Determination of Dissociation Constants. Equilibrium constants for hybridization of antisense oligonucleotides to the RNA hairpin were measured using a gel shift assay (Pyle et al., 1990; Ausubel et al., 1989; Fried & Crothers, 1981; Garner & Revzin, 1981; Pontius & Berg, 1991; Revzin, 1989; Bhattacharyya et al., 1990). Hybridization reactions were prepared in 20 μL containing 100 mM Na^+, 10 mM phosphate, pH 7.0, 1000 cpm of 5′-^{32}P-labeled transcript and antisense oligonucleotide ranging in concentration from 1 pM to 10 μM and incubated 20 h at 37 °C. After addition of 10 μL of loading buffer (15% Ficoll, 0.25% bromphenol blue, and 0.25% xylene cyanole FF), reactions were resolved at 10 °C in a 12% native polyacrylamide gel containing 44 mM Tris–borate and 1 mM $MgCl_2$. Hybridization of antisense oligonucleotides to complementary oligonucleotide targets was measured similarly except resolution was on a native 20% polyacrylamide gel. Gels were quantitated using a Molecular Dynamics Phosphorimager. If the antisense oligonucleotide concentration substantially exceeds the target concentration, the dissociation constant (K_d) is simply the antisense oligonucleotide concentration at which 50% of the target is shifted. Due to the limited specific activity of the targets, concentrations were roughly 25 pM for the transcript and 8 pM for the oligonucleotide target so association constants tighter than 1.5×10^{10} M^{-1} for the 47-mer or 5×10^{11} M^{-1} for the 10-mer could not be accurately measured.

Determination of Hybridization Rates. To measure bimolecular association rates (k_1), hybridization reactions were prepared as described above except a single antisense oligonucleotide concentration (10-fold over the K_d) was used. Reactions were incubated at 37 °C for prescribed intervals and quenched by snap-freezing on dry ice. Reactions were individually thawed and immediately loaded onto a running native polyacrylamide gel.

To determine dissociation rates, the concentration of antisense oligonucleotide used in the k_1 determination was incubated with the labeled target RNA for 20 h at 37 °C. Following annealing, unlabeled target was added in 10-fold excess to the antisense oligonucleotide, and reactions were incubated at 37 °C for the prescribed intervals. Reactions were snap-frozen and analyzed on polyacrylamide gels as described above.

RESULTS

Structure Map of the mRNA Hairpin. The enzymatic structure map for the 47-mer transcript corresponding to residues 18–64 of mutant Ha-*ras* mRNA is shown in Figures 1a and 2 (lanes 2–4). To ensure only primary cleavage sites were detected, both 3′ and 5′ end-labeled transcripts were tested (Douthwaite & Garrett, 1981). Only cleavage sites detected with both labelings are reported in Figure 1a.

Enzymatic structure mapping of the 47-mer transcript reveals a hairpin structure consisting of either a 12 base pair stem and a 19-membered loop or a 13 base pair stem with a 16-membered loop. The ambiguity in the stem size is due to digestion of the C(33)-G(50) base pair with both double- and single-strand-specific enzymes. Mapping data from both the 5′ and 3′ end-labeled substrates demonstrate these are primary hits, suggesting this base pair is transitory and both conformations are present.

A weak double-strand-specific primary hit was observed within the loop at A(47). The presence of strong single-stranded hits on either side of this residue and the absence of complementary sequences anywhere else in the fragment suggest this V1 cleavage site is an artifact of enzymatic structure mapping.

Association Constants for Hybridization of Antisense Oligonucleotides to the RNA Hairpin. Table I describes six decaribonucleotides for which dissociation constants were measured. Two, 3270 and 3271, are complementary to the stem region of this hairpin; one, 3292, is partially complementary to the stem and partially complementary to the loop;

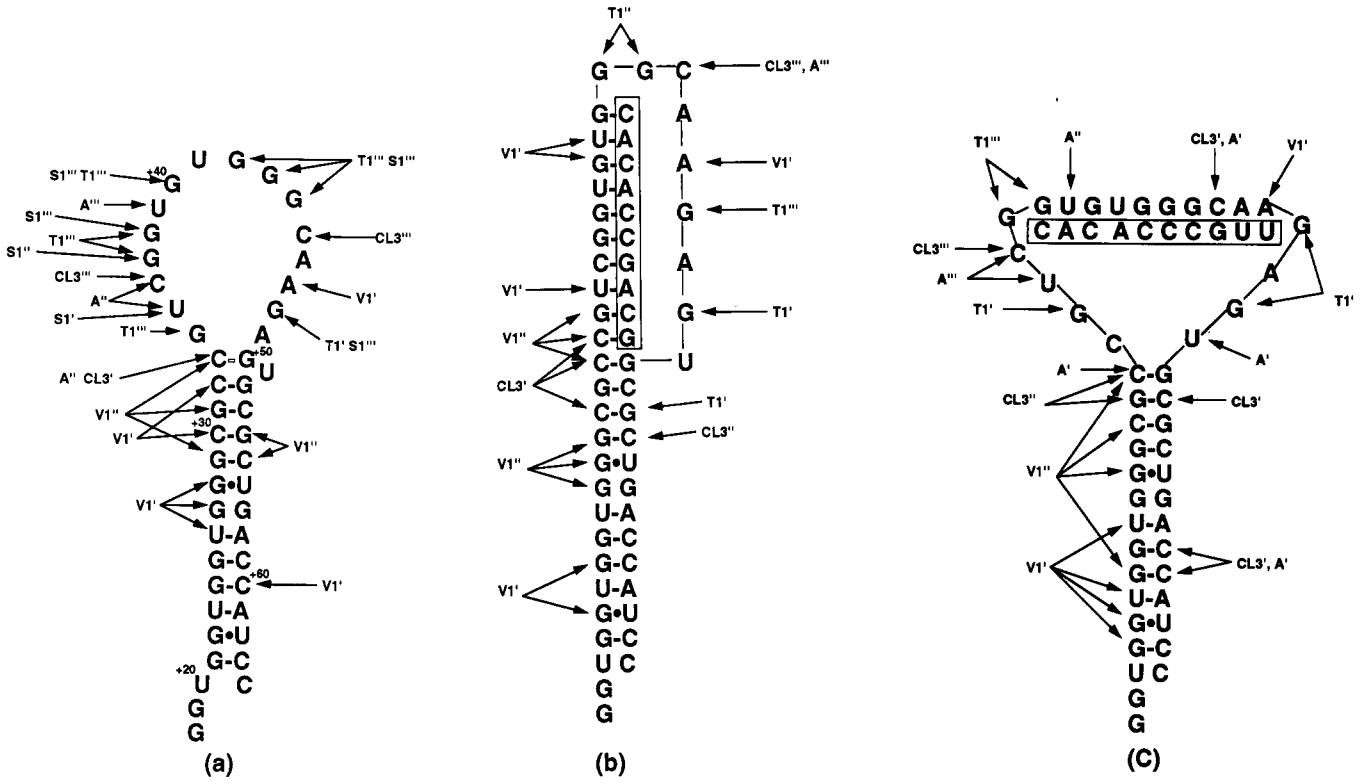

FIGURE 1: Enzymatic structure maps of (a) the 47-mer fragment corresponding to residues 18–64 of mutant Ha-*ras* mRNA, (b) the 47-mer transcript bound to 3291, and (c) the 47-mer transcript bound to 3283. The degree of digestion is indicated by the superscript prime (one prime = weak; three primes = strong). Specificity for each enzyme is as follows: RNase V1 primarily cleaves double-stranded regions irrespective of sequence; RNase T1 recognizes single-stranded regions and cleaves Gp↓N bonds; RNase A primarily recognizes single-stranded pyrimidines and cleaves Yp↓N bonds. RNase CL3 primarily cleaves after single-stranded cytidine, and RNase S1 cleaves single-stranded regions indiscriminately.

the others target the 5′ side (3291), the middle (3283), and the 3′ side (3284) of the loop.

For each antisense oligonucleotide, dissociation constants were measured using the gel shift assay. Figure 3 plots percent target shifted as a function of antisense concentration for each antisense oligonucleotide and each of two targets, the 47-mer hairpin and a complementary single-stranded RNA 10-mer. Association constants (K_a) determined from these curves are listed in Table I. For 3291 hybridizing to the hairpin target, the apparent K_d is 4×10^{-11} M, a concentration only slightly larger than that estimated for the target. Therefore, this association may be stoichiometrically limited, and the association constant may be greater than the value listed in Table I.

The three antisense oligonucleotides targeted to the stem region of the hairpin exhibited 10^5–10^6-fold lower affinity for the hairpin target than for the length-matched dodecamer target. For the three oligonucleotides targeted to the loop, the thermodynamic effect of the hairpin depends on the target site. 3284, targeted to the 3′ side of the loop, binds substantially less favorably to the hairpin than to its complementary 10-mer. 3283, targeted to the middle of the loop, binds 10-fold less favorably to the hairpin than to the complementary 10-mer, and 3291, targeted to the 5′ side of the loop, binds at least as favorably to the hairpin as to its 10-mer complement. Although reproducibility in K_a's measured by gel shift is no better than 2-fold, the plot in Figure 3D and the kinetic data presented below suggest that 3291 binds slightly more tightly to the hairpin than to its length-matched complement.

To confirm measured equilibrium constants reflect hybridization conditions, not electrophoresis conditions, assays were performed using different loading and running buffers for the gel electrophoresis. No change in the K_d was observed. In addition, the K_d for hybridization of a biotinylated oligonucleotide was determined by capture and separation using streptavidin-conjugated magnetic beads (Ito et al., 1992). The K_d determined using this alternate method of separation agreed well with that determined by the gel shift assay, demonstrating that the gel shift technique is measuring equilibrium under the hybridization conditions.

Migrational Retardation of the Hybrid. For all six decaribonucleotides, hybridization of the oligonucleotide to the hairpin target reduced the mobility of the hairpin on the native polyacrylamide gel. The degree of retardation ranged from 3 mm for 3291 ($K_a \geq 3 \times 10^{10}$ M^{-1}) to 12 mm for 3284 ($K_a < 1 \times 10^5$ M^{-1}). As shown in Figure 4, the degree of retardation correlates inversely with the association constant for this interaction.

Structure Map of the Hybrid. Structure maps for 3291 and 3283 bound to the hairpin are shown in Figures 1b, 1c, and 2 (lanes 6–8, 10–12). In each case, upon hybridization, strong single-stranded hits at the target site in the transcript disappear and are replaced by double-strand-specific hits in the hybrid. For 3291, digestion patterns for regions outside the target site are virtually identical for both the hybrid (Figure 1b) and the unbound transcript (Figure 1a). In contrast, for 3283, digestion patterns outside the target site differ for the hybrid (Figure 1c) and the unbound transcript (Figure 1a). Compared to the free transcript, the hybrid shows reduced digestion with RNase T1 at G(34) and enhanced digestion with RNase A at U(35) and C(36). Both hybrid maps also show double-strand- and single-strand-specific hits at the top of the stem, suggesting that this region is destabilized by formation of the hybrids.

Rate Constants for Hybridization of Antisense Oligonucleotides to the RNA Hairpin. Bimolecular association rate

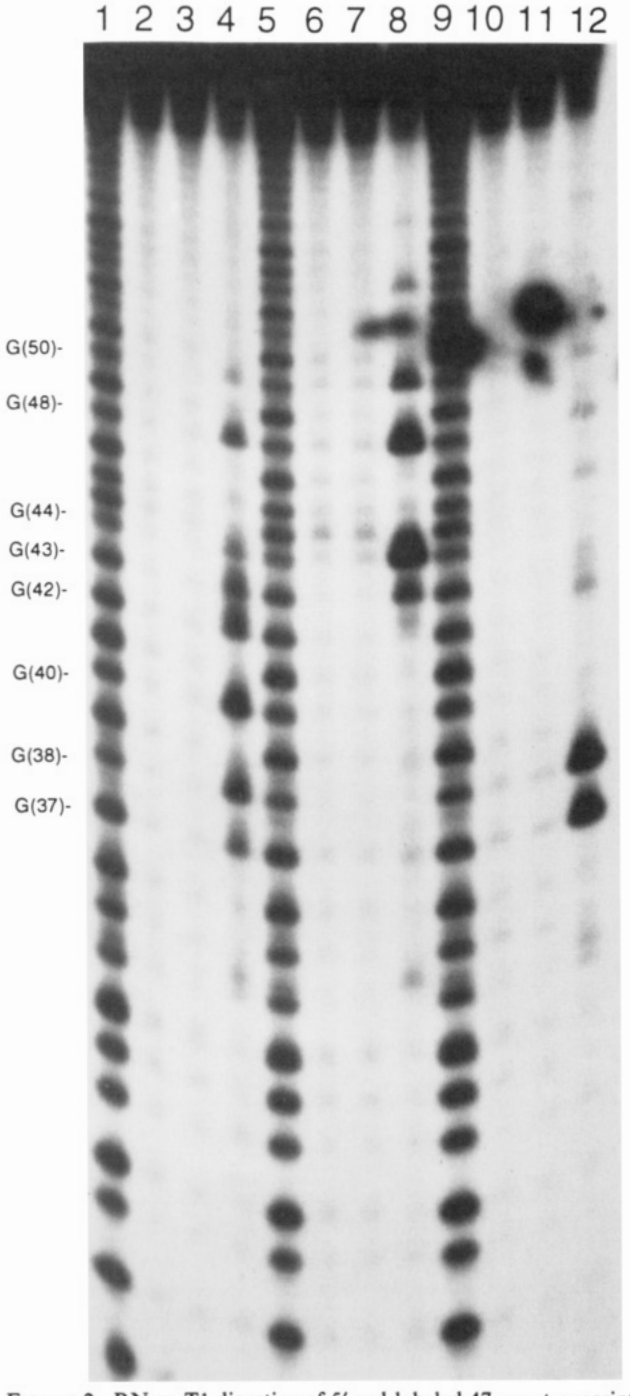

FIGURE 2: RNase T1 digestion of 5′ end-labeled 47-mer transcript with no oligonucleotide added (lanes 2–4), hybridized to 3291 (lanes 6–8), or hybridized to 3283 (lanes 10–12). Digestions were performed as described with 0.9 unit of RNase T1 (lanes 2, 6, and 10), 1.2 units of RNase T1 (lanes 3, 7, and 11), or 1.5 units of RNase T1 (lanes 4, 8, and 12). The base hydrolysis ladder (lanes 1, 5, and 9) was prepared by incubation of 5′ end-labeled transcript at 90 °C for 5 min in 10 μL containing 100 mM sodium carbonate, pH 9.0.

constants (k_1) and dissociation rate constants (k_{-1}) for three oligonucleotides to each target are listed in Table II. Association rates were calculated from the measured dissociation rate and the measured equilibrium constant, $K_a = k_1/k_{-1}$. Some association rates were also measured directly. In those cases, experimental and calculated rates correlated well.

Trends observed for k_1 are similar to those noted above for K_a; hybridization rates for 3283 and 3291 are similar for both the hairpin and single-stranded targets. In contrast, 3292, which targets some stem and some loop, hybridizes 10^7-fold more slowly to the hairpin than to the short single-stranded target. Dissociation rates, on the other hand, are similar for both the hairpin and short single-stranded targets.

Due to the low affinity of 3292 for the 47-mer target, a large concentration of unlabeled target was required to capture dissociated antisense oligonucleotide. Therefore, this dissociation rate was determined using unlabeled 10-mer target rather than unlabeled 47-mer target to capture dissociated antisense oligonucleotide. To confirm that use of unlabeled 10-mer target did not affect the measured dissociation rate, dissociation rates for 3291 and 3283 from 47-mer target were measured using both unlabeled 47-mer and unlabeled 10-mer as capture RNAs. Dissociation rates were unaffected by the length of the unlabeled capture RNA.

DISCUSSION

Thermodynamic Results Suggest Structured Single-Stranded Regions Impact Antisense Binding as Effectively as Double-Stranded Regions. The impact target secondary structure exhibits on antisense oligonucleotide binding is demonstrated by the difference between K_a's for the oligonucleotide–hairpin hybrids and the oligonucleotide–oligonucleotide complexes (last column in Table I). For oligonucleotides targeted to the stem of the hairpin, binding to the hairpin is 10^5–10^6-fold less favorable than binding to a 10-mer target. This difference is likely due to the requirement that base pairs in the stem must be disrupted before the antisense oligonucleotide can bind. In contrast, no significant secondary structure need be disrupted in the single-stranded target. For example, thermodynamic parameters for RNA folding (Jaeger et al., 1989) predict disruption of stem residues necessary to bind 3292 requires +8.9 kcal/mol, thus predicting the antisense oligonucleotide will bind 5×10^{-7}-fold as well to the hairpin as to single-stranded 10-mer target. Considering ionic conditions for the prediction and the experiment differ, the observed ratio of 4×10^{-6} for 3292 supports this simple interpretation.

For the three oligonucleotides targeted to the loop, the thermodynamic effect of the hairpin depends on the target site. These effects cannot be explained by simple base-pairing thermodynamics. For all three antisense oligonucleotides, the target site is single-stranded as evidenced by cleavage with single-strand-specific nucleases, and no base pairs should have to be broken for hybridization to occur. Clearly, the loop structure must be responsible for this effect. It appears the thermodynamic cost of binding to residues 43–52 is similar to that of binding to a stem region. Binding to residues 33–42, on the other hand, has a small negative cost; it is slightly easier to bind to the loop structure than the free single strand.

Similar results have been observed for binding of short antisense oligonucleotides to hairpin loops in tRNA (Uhlenbeck, 1972; Freier & Tinoco, 1975); oligonucleotides targeting the 5′ side of the anticodon loop bind more tightly to the hairpin loop than to their single-stranded complements (Uhlenbeck, 1972). Binding to the 3′ side of the loop, however, is not observed.

Retardation Distances Support the Thermodynamic Results. Migrational differences between the hybrid and the free transcript are an additional indication that the loop structure is responsible for the difference in binding behavior for antisense oligonucleotides targeted to the loop. One factor contributing to migrational retardation of the hybrid is conformational changes in the transcript due to hybrid formation. In situations where hybridization results in significant perturbation of target secondary structures, the effect on migration of the hybrid band would be greater

Table I: Association Constants for Six Antisense Oligonucleotides Hybridizing to a 47-mer Hairpin Target and Single-Stranded Complementary 10-mer Targets[a]

	oligonucleotide	complementary residues in hairpin target	K_a, hairpin target (M^{-1})	K_a, single-stranded oligonucleotide target (M^{-1})	ratio[b]
stem	3270	18–27	1×10^5	3×10^{10}	3×10^{-6}
stem	3271	23–32	1×10^6	1×10^{11}	1×10^{-5}
loop	3292	28–37	2×10^5	5×10^{10}	4×10^{-6}
loop	3291	33–42	$\geq 3 \times 10^{10}$	2×10^{10}	≥ 1.5
loop	3283	38–47	2×10^9	2×10^{10}	1×10^{-1}
loop	3284	43–52	$<1 \times 10^5$	2×10^{10}	$<5 \times 10^{-6}$

[a] Hybridization conditions are given in the text. Estimated errors are ± a factor of 2. [b] Ratio of K_a for the 47-mer hairpin target to K_a for a single-stranded 10-mer target.

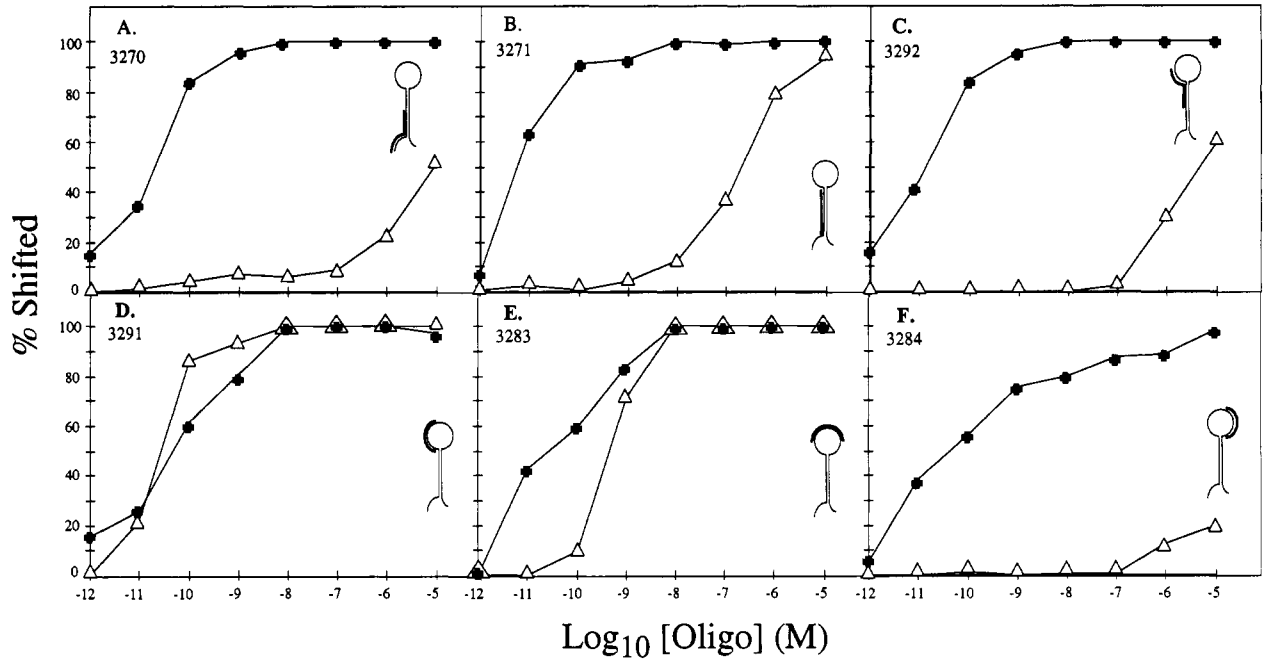

FIGURE 3: Fraction of target shifted vs concentration of antisense oligonucleotide for the six antisense oligonucleotides described in Table I binding to the 47-mer hairpin target (△) or to a single-stranded complementary decaribonucleotide target (●). (A) 3270; (B) 3271; (C) 3292; (D) 3291; (E) 3283; (F) 3284. The double line in the schematic indicates the target site for each oligonucleotide.

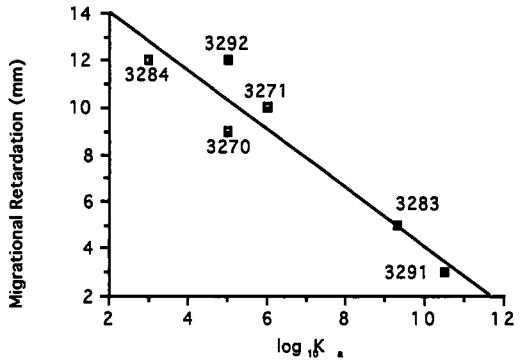

FIGURE 4: Gel retardation for each oligonucleotide binding to the hairpin loop vs the association constant of this interaction. The ordinate reports the distance between free and bound transcript. Under the electrophoresis conditions used, free transcript migrated 110 mm. The K_a for 3284 was extrapolated from gel shift data at 100 μM oligonucleotide.

retardation. Data in Figure 4 support this hypothesis; three oligonucleotides targeted to the stem as well as 3284 show large retardation on the gel. In contrast, binding of 3291 shows the most favorable thermodynamic effect of hairpin structure and the smallest retardation on the gel.

Thermodynamic and Gel Retardation Results Suggest a Model for the Loop Structure. Model building of the hairpin reveals that steric constraints limit the number of nucleotides that can stack on the 5′ side of the loop to 11, terminating with G(43). As shown in Figure 5a, the remaining unstacked region must be long enough to span the stacked single-stranded helix and allow for formation of the stem. Therefore, the target site for 3291 would fall within the proposed stacked region while the target site for 3283 would continue past G(43).

Figure 5c shows that under the proposed model, hybridization of 3283 to the transcript would result in distortion of the loop structure. In contrast, hybridization of 3291 (Figure 5b) requires no change in the loop structure. The larger retardation and weaker K_a observed for 3283 compared to 3291 are consistent with this model. The large retardation and very weak K_a of 3284 are also consistent with the proposed model because hybridization would require substantial conformational change.

Structure Map of the Hybrid Is Consistent with the Model. Further validation of the proposed model is illustrated by structure maps for the 3291 and 3283 hybrids. Digestion patterns outside of the target site for the free hairpin and the 3291 hybrid are virtually identical and therefore consistent with no conformational changes in the hairpin upon binding of 3291. The change in digestion patterns outside of the target site upon binding of 3283 is consistent with a hybridization-induced conformational change in this region.

Effects of Structure on Hybridization Kinetics. Data in Table II demonstrate thermodynamic trends noted above are due to trends in the association rate. Whereas dissociation

Table II: Rate Constants for Three Antisense Oligonucleotides Hybridizing to a 47-mer Hairpin Target and Single-Stranded Complementary 10-mer Targets[a]

	oligonucleotide	observed[b]		calculated[c]	ratio[d]
		k_{-1} (s^{-1})	k_1 (M^{-1} s^{-1})	k_1 (M^{-1} s^{-1})	
47-mer target	3292	1×10^{-4}	13	19	10^{-7}
	3291	2×10^{-2}		$\geq 2 \times 10^{8}$	≥ 2.5
	3283	1×10^{-2}	6×10^{6}	1×10^{7}	0.25
10-mer target	3292	4×10^{-3}		2×10^{8}	
	3291	2×10^{-2}	1×10^{7}	8×10^{7}	
	3283	2×10^{-2}		4×10^{7}	

[a] Hybridization conditions are given in the text. Antisense oligonucleotides are described in Table I. Estimated errors are ± a factor of 2. [b] Rates were determined experimentally as described under Materials and Methods. [c] Association rate was calculated from the measured dissociation rate and the measured equilibrium constant. [d] Ratio of k_1 for the 47-mer hairpin target to k_1 for a single-stranded 10-mer target.

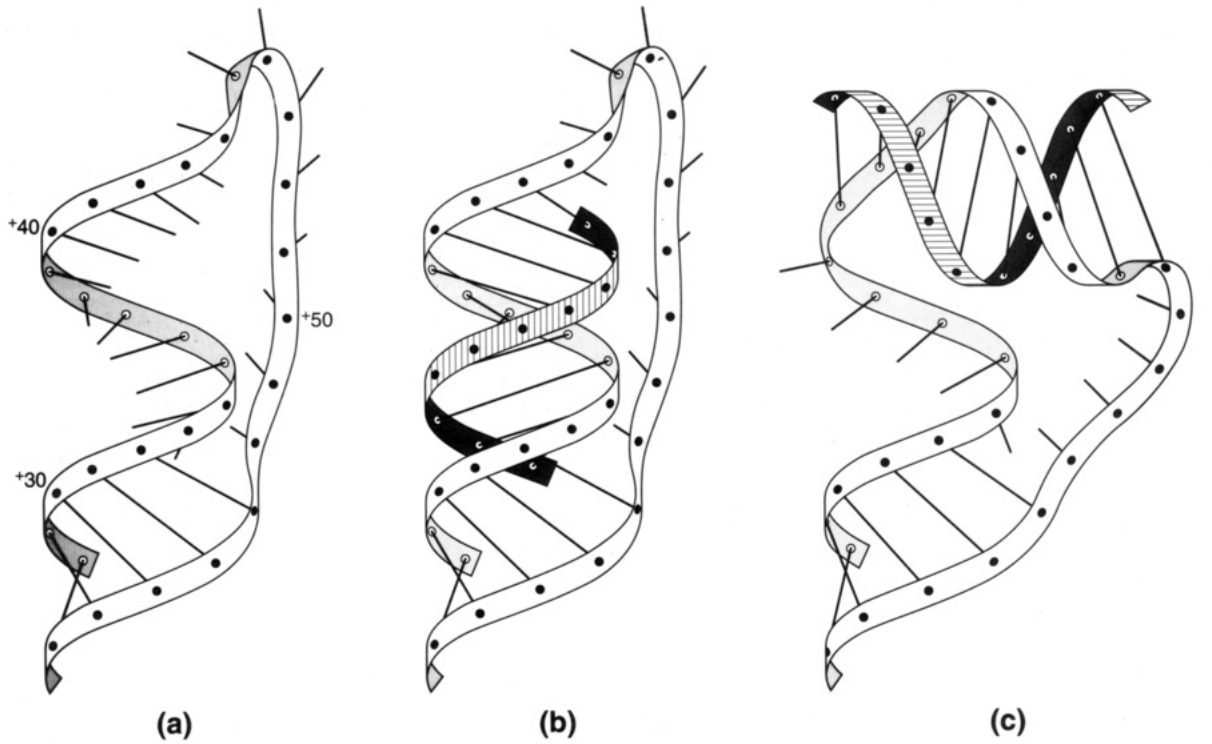

FIGURE 5: Proposed structures for (a) the unbound 47-mer transcript, (b) the hybrid of 3291 and the 47-mer transcript, and (c) the hybrid of 3283 and the 47-mer transcript.

rates are similar for both targets and all three oligonucleotides studied, association rates vary from 10^1 to 10^8 M^{-1} s^{-1}. That target structure plays an important role in association rates is demonstrated by the difference in association rates for the hairpin target compared to a single-stranded 10-mer target (last column in Table II). 3292, targeted partially to the stem and partially to the loop, binds 10^7 times more slowly to the hairpin than to a single-stranded 10-mer target. In contrast, 3291, targeted to the 5′ side of the loop, binds faster to the hairpin than to a single-stranded target. These data continue to support the model that the loop structure promotes hybridization on the 5′ side of the loop. In fact, the k_1 for binding 3291 to the hairpin is approximately 10-fold faster than association rates reported for other structured RNA hybrids (Yoon et al., 1975; Fedor & Uhlenbeck, 1990; Chow et al., 1992), supporting the notion that a particularly favorable loop structure is involved.

Implications for Design of Antisense Oligonucleotides. These data indicate the tightest binding of antisense oligonucleotides occurs at target sites for which disruption of the target structure is minimal. Therefore, considerations of the target secondary structure dictate single-stranded regions should be selected over double-stranded regions. Furthermore, due to the loop structure, not all single-stranded regions exhibit structures favorable to hybridization. Once single-stranded regions are identified, the ideal target site must be determined empirically.

Long single-stranded regions such as the loop region in this 47-mer fragment of mutant Ha-*ras* mRNA have been observed in other RNAs (White & Draper, 1989) but may be rare. Therefore, attempts should be made to keep oligonucleotide length to a minimum. This can be achieved by use of modified antisense oligonucleotides such as 2′-*O*-methyl derivatives that exhibit a higher affinity than unmodified DNA for target RNAs (Freier et al., 1992). In addition, inherently greater affinity obtained from targeting ideally structured regions eliminates the need for increased oligonucleotide length.

Selecting target sites favorable for hybridization may also help increase the specificity of an antisense oligonucleotide. If the target sequence occurs elsewhere, it is unlikely to be in such a favorable conformation. Thus, affinity to the incorrect site will be reduced, and specificity of the antisense oligonucleotide will be maximized.

Significance to Antisense Targeting of Ha-ras. On the basis of the above results, predictions can be made regarding the design of antisense oligonucleotides against mutant Ha-*ras* mRNA. Activation of the Ha-*ras* oncogene has been shown to occur through mutations in its coding sequences

(Barbacid, 1987). Presumably, inhibition of expression of the mutation-carrying gene is desired without affecting expression of the normal gene which is generally believed to be essential for cell survival. Therefore, directing oligonucleotides to mutations within the Ha-*ras* mRNA may be desirable.

We show here that targeting residues 33–43 of Ha-*ras* mRNA containing a codon 12 activating point mutation (GGC → GUC) should result in high affinity and therefore high antisense activity. The results suggest shifting the target site from residues 33–43 in either direction should reduce affinity and therefore activity. Modeling suggests only 11 nucleotides of the loop are stacked; therefore, increasing the length of the antisense oligonucleotide above 11 may not increase activity. Experiments on the analogous fragment from wild-type Ha-*ras* mRNA show it too forms a hairpin structure with similar patterns of antisense binding (W. F. Lima, unpublished results). Thus, selective targeting of mutant over wild-type Ha-*ras* mRNA should be possible with an oligonucleotide as short as 11 nucleotides. These predictions assume in vivo binding to full-length *ras* mRNA (973 residues) follows patterns observed in vitro for the 47-mer fragment. Folding predictions (Jaeger et al., 1989) on full-length exon 1 (mRNA residues −51 to 104) support this assumption. Experiments to test these hypotheses are in progress.

In summary, mRNA structure influences the affinity of antisense oligonucleotides by affecting association rates. In this hairpin system, with a big single-stranded loop, the stem structure reduced the affinity of oligonucleotides targeted to the stem. Surprisingly, targeting the single-stranded loop region did not always result in high affinity. Due to structure in the loop, targeting the 3′ side of the loop was as ineffective as targeting the stem while targeting the 5′ side of the loop resulted in affinity even higher than that for a single-stranded 10-mer target. Due to the observed effect of loop structure on hybridization affinities, design of effective antisense oligonucleotides will require consideration of target tertiary as well as secondary structure.

ACKNOWLEDGMENT

We thank Maryann Zounes for oligonucleotide synthesis and Drs. Olke Uhlenbeck and Christopher Mirabelli for helpful discussions.

REFERENCES

Ausubel, F. M., Brent, R., Kingston, R. E., Moore, D. D., Seidman, J. G., Smith, J. A., & Struhl, K. (1989) in *Current protocols in molecular biology*, John Wiley, New York.

Bacon, T. A., & Wickstrom, E. (1991) *Oncogene Res. 6*, 13.

Barbacid, M. (1987) *Annu. Rev. Biochem. 56*, 779.

Bhattacharyya, A., Murchie, A. I. H., & Lilley, D. M. (1990) *Nature 343*, 484.

Chiang, M.-Y., Chan, H., Zounes, M. A., Freier, S. M., Lima, W. F., & Bennett, C. F. (1991) *J. Biol. Chem. 266*, 18162.

Chow, S. A., Chiu, S.-K., & Wong, B. C. (1992) *J. Mol. Biol. 223*, 79.

Douthwaite, S., & Garrett, R. A. (1981) *Biochemistry 20*, 7301.

Fedor, M. J., & Uhlenbeck, O. C. (1990) *Proc. Natl. Acad. Sci. U.S.A. 87*, 1668.

Freier, S. M., & Tinoco, I., Jr. (1975) *Biochemistry 14*, 3310.

Freier, S. M., Alkema, D., Sinclair, A., Neilson, T., & Turner, D. H. (1985) *Biochemistry 24*, 4533.

Freier, S. M., Lima, W. F., Sanghvi, Y. S., Vickers, T., Zounes, M., Cook, P. D., & Ecker, D. J. (1992) in *Gene regulation: Biology of antisense RNA and DNA* (Erickson, R. P. & Izant, J. G., Eds.) pp 95–107, Raven Press, New York.

Fried, M., & Crothers, D. M. (1981) *Nucleic Acids Res. 9*, 6505.

Garner, M. M., & Revzin, A. (1981) *Nucleic Acids Res. 9*, 3047.

Gutell, R. R., Weiser, B., Woese, C. R., & Noller, H. F. (1985) *Prog. Nucleic Acid Res. Mol. Biol. 32*, 155.

Herschlag, D., & Cech, T. R. (1990a) *Biochemistry 29*, 10159.

Herschlag, D., & Cech, T. R. (1990b) *Biochemistry 29*, 10172.

Ito, T., Smith, C. L., & Cantor, C. R. (1992) *Proc. Natl. Acad. Sci. U.S.A. 89*, 495.

Jaeger, J. A., Turner, D. H., & Zuker, M. (1989) *Proc. Natl. Acad. Sci. U.S.A. 86*, 7706.

Jinno, Y., Merlino, G. T., & Pastan, I. (1988) *Nucleic Acids Res. 16*, 4957.

Pontius, B. W., & Berg, P. (1991) *Proc. Natl. Acad. Sci. U.S.A. 88*, 8237.

Pyle, A. M., McSwiggen, J. A., & Cech, T. R. (1990) *Proc. Natl. Acad. Sci. U.S.A. 87*, 8187.

Reddy, E. P. (1983) *Science 220*, 1061.

Revzin, A. (1989) *BioTechniques 7*, 346.

Sambrook, J., Fritsch, E. F., & Maniatis, T. (1989) in *Molecular Cloning. A Laboratory Manual*, 2nd ed., Cold Spring Harbor Laboratory Press, Cold Spring Harbor, NY.

Uhlenbeck, O. C. (1972) *J. Mol. Biol. 65*, 25.

White, S. A., & Draper, D. E. (1989) *Biochemistry 28*, 1892.

Wickstrom, E., Simonet, W. S., Medlock, K., & Ruiz-Robles, I. (1986) *Biophys. J. 49*, 15.

Wu, T., Ogilvie, K. K., & Pon, R. T. (1989) *Nucleic Acids Res. 17*, 3501.

Wu, T., & Ogilvie, K. K. (1990) *J. Org. Chem. 55*, 4717.

Yoon, K., Turner, D. H., & Tinoco, I., Jr. (1975) *J. Mol. Biol. 99*, 507.